Investigation of a Helium cooling circulation loop on a 1.3 GHz cavity structure

M Chioteli [1*], H. Constantinou [2], A. Onufrena [3], and T. Koettig [4]

[1,2,3,4] Technology department, CERN, Geneva, Switzerland

[*]E-mail: maria.chioteli@cern.ch

Abstract. This paper presents a novel cryogenic cooling method for Superconducting Radio Frequency (SRF) cavities, utilizing a cold helium flow passed through a brazed capillary for their cooling. Such novel and drastically reduced helium content cooling scheme can be applied to a wide variety of superconducting cavities, and it has many advantages compared to the traditional cooling method of SRF cavities in a liquid helium bath. The paper describes cooling options and configurations concerning helium forced flow heat transfer at the capillary surface plus the resulting temperature distribution in the cavity itself.

The results from the cold commissioning of the experimental system are outlined, demonstrating that the cavity could reach a minimum temperature of 6.5 K with an applied heat load of 1 W, with a He circulation loop based on a 1.8 W @ 4.2 K cryocooler. A LHe booster heat exchanger has been introduced to achieve even lower temperatures and ensure consistent inlet conditions for further evaluation of cavity cooling efficiency. The upgraded setup allows to apply up to 7 W heat load in the 1.3 GHz Cu cavity and reaching stable operating conditions below 6.5 K.

1. Introduction

In remote cooling systems, the cooling power source is separated from the cooled object, either mechanically or by distance. Cryocoolers provide the necessary cooling power in combination with a closed fluid circulation loop, enabling standalone operation and eliminating the need for extensive cryogenic infrastructure to maintain a continuous supply of liquid cryogens. Remote systems aim to enhance cryocooler-based cooling power and facilitate heat extraction across larger areas at the cooling interface. Moreover, compared to traditional methods involving liquid helium baths, remote systems use less fluid, reducing the potential risk of leaks into the cryostat and minimizing associated safety hazards. One promising application for remote cooling systems is in the cooling of Superconducting Radio-Frequency (SRF) cavities (Dry cavity cooling), currently cooled within helium baths at temperatures below 4.5 K [1].

An SRF cavity is a crucial component in the Large Hadron Collider (LHC) at CERN as it is the one that accelerates the protons to extremely high energies and speeds. They are made by superconducting materials, because of their unique property of zero electrical resistance when cooled down to low temperatures. The state-of-the-art material for SRF cavities is high-purity niobium, coated as a thin layer inside a Cu cavity. However, Nb_3Sn has emerged as an alternative in recent years due to its higher critical temperature (18 K compared to niobium's 9.2 K), reducing the need for extremely low-temperature cooling [2,3].

2. Experimental setup

During the commissioning, two test campaigns were conducted. The first one involved testing the system and cooling the cavity by a cryocooler alone, referred to as "cryocooler standalone operation". The second one utilized a booster heat exchanger along with an additional 4.2 K liquid helium bath, referred as "booster heat exchanger integrated operation", intended to provide additional cooling power to the cavity.

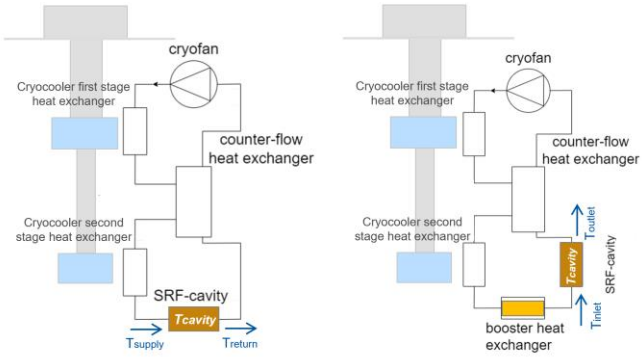

Figure 1. Left: "Cryocooler standalone operation". Right: "Booster heat exchanger integrated operation".

A schematic representation of the designed remote cooling system for the "cryocooler standalone operation" is depicted in Figure 1 on the left. In this deployed system, the SRF cavity is cooled using a two-stage cryocooler with an additional helium circulation loop. The helium flow is circulated by the cryofan and passes through a counter-flow heat exchanger (CFHEX), as well as through the heat exchangers of the cryocooler stages. The high-effectiveness CFHEX facilitates the operation of such cooling loops by enhancing the efficiency of heat transfer within the system [4]. In details, upon exiting the first stage of the cryocooler, the flow continues through the CFHEX, utilizing the lower temperature of the returning flow from the SRF cavity. The performance of the 2nd stage of the cryocooler determines the fluid temperature at the inlet of the cavity (donated as T_{supply}). The proposed cooling interface (CIF) between the cooled fluid and the cavity is achieved via a helically wound thin capillary tube which is soldered onto the outer shell of the cavity as depicted in Figure 2 on the left.

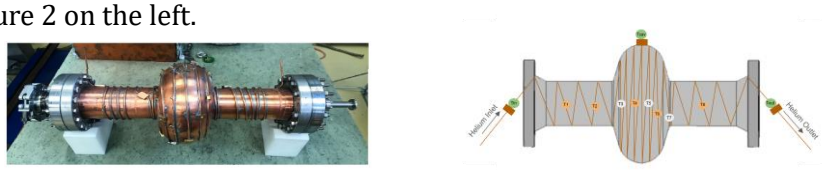

Figure 2. Left: Mock-up 1.3 GHz Cu cavity with the soldered capillary tube (inner diameter 2 mm, length 8 m). Right: Distribution of each temperature sensor on the cavity.

In the case of the SRF cavity (Nb_3Sn coatings), the system should be able to ensure a cavity temperature below 8 K at mass flow rates between 100 mg/s and 500 mg/s. Furthermore, operating pressures of 1.1 bar (two-phase flow conditions) and 3-10 bar (supercritical conditions) should be studied. The two-stage pulse-tube cryocooler can provide 1.8 W at 4.2 K with 65 W @ 45 K at the respective stages with an electrical consumption of 11 kW. Regarding the "booster heat exchanger integrated operation", the additional booster heat exchanger is installed upstream of the cavity, as shown in Figure 1 on the right. This booster heat exchanger operates

within a 4.2 K liquid helium bath, providing the necessary cooling to achieve a lower and constant inlet temperature, and consequently a lower cavity temperature with higher possible heat loads.

3. Experimental procedure

A wide range of parameters influence the performance of the whole system and the capillary CIF, particularly in terms of heat transfer capabilities and pressure drop. These parameters include the capillary's diameter and length, the phase of the fluid flow, vapor quality (in the case of two-phase flow), system operating conditions, and the heat applied to it or any residual heat loads. At first, numerical simulations were conducted in order to determine the initial geometry of the CIF and its impact on the CIF performance. These simulations, detailed in reference [1], identified the optimal capillary dimensions for the mock-up cavity, focusing on achieving the best pressure drop and temperature gradient for a 2 W heat load. As a result, a capillary length of 8 meters and an inner diameter of 2 millimetres were selected. Additionally, considering a typical heat load profile due to Radio Frequency (RF) losses, the temperature profile along the cavity under various flow conditions was analysed [1]. Afterwards, cold commissioning and thermal characterization of the experimental system with the mock-up cavity were carried out. The aim was to evaluate the system's performance by varying the cryofan speed and pressure in order to understand their impact on mass flow, temperatures and pressure drops throughout the entire system. Flow phase conditions and system stability were also evaluated.

Specifically, the "cryocooler standalone operation" study aimed to evaluate the overall system performance, including the cryocooler's efficiency, the effectiveness of the counter-flow heat exchanger, the influence of cryofan speed and pressure on the mass flow rate and temperatures, and potential heat loads affecting the system. The "booster heat exchanger integrated operation" study focused primarily on the cavity's cooling performance and temperatures rather than the entire system. In both cases, pressures above supercritical conditions were mainly studied, with an emphasis on pressures ranging between 3-6 bar and 9-10 bar. Supercritical helium was chosen due to its low pressure drop and predictable behaviour, as it lacks the complexities associated with two-phase flow effects. Finally, a halogen lamp with a resistance of 7 Ω was installed at the center of the mock-up cavity to mimic uniform heating as expected from RF loads. This aimed to introduce a heat load and assess its influence on the flow and the temperatures within the system and the cavity. Measurements were conducted with different heating power settings ranging from 0 to 1 W during the cryocooler standalone operation and from 0 to 7 W during the booster heat exchanger integrated operation.

4. Results

4.1 Cryocooler standalone operation

During the cryocooler standalone operation, the system was tested by varying the cryofan speed and the pressure of the system in order to assess the mass flow capabilities, possible instabilities, the system's reaction, and determine what temperatures could be achieved throughout the system and the cavity. For no introduced heat load, the lowest supply temperature to the cavity, denoted as T_{supply} in Figure 1, which is the temperature measured after the second stage of the cryocooler, was 3.80 K ± 20 mK. This temperature is indicative not only of the cryocooler's performance but also of the overall system performance, including the contributions from the two stages of the cryocooler and the *CFHEX*. For this supply temperature, the lowest temperature achieved at the equator of the cavity, denoted as T_{cavity}, was 4.12 K ± 20 mK. This was achieved with a mass flow

of approximately 80 mg/s ± 15-20%, a pressure of 2.9 bar and a cryofan speed of 4800 rpm. Subsequently, increasing the mass flow rate, by raising the cryofan speed and He pressure, led to an increase in the supply temperature, which in turn resulted in higher cavity temperatures as well. This occurs because increasing the mass flow rate introduces higher heat loads to the system, elevating the temperatures. On the other hand, higher mass flow rates enhance the heat transfer between the helium flow and the cavity. However, beyond a certain threshold, it was noticed that further increases in mass flow rate become less effective, particularly when achieved with higher pressures and temperatures. This occurs because when the system operates far from the supercritical point, heat transfer efficiency decreases in the capillary. Therefore, it is essential to identify an optimal range of parameters that balances these effects for optimal system performance. Furthermore, to assess the impact of the introduced heat load on the flow and temperatures within the system and the cavity, measurements were conducted under some representative conditions with different pressures and mass flow rates. These measurements were taken with various heating power settings ranging from 0 to 1 W.

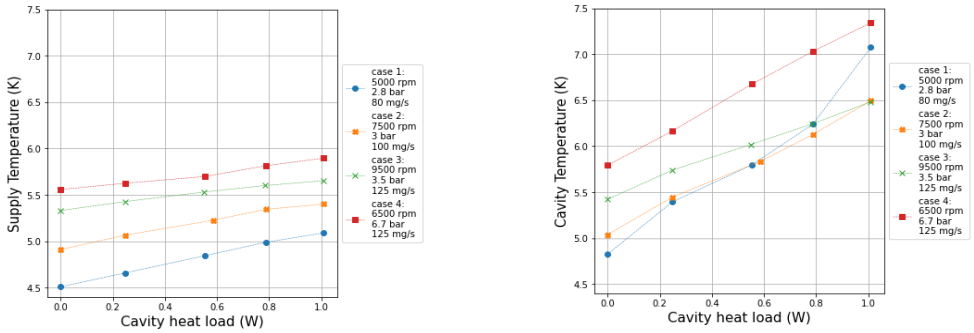

Figure 3. Left: Supply temperature at each heat load level for the four different cases. Right: Cavity temperature at each heat load level for the four different cases.

Figure 3 on the left depicts a comparison of the supply temperature at each heat load level for the four different cases, while Figure 3 on the right depicts a comparison of the temperature at the cavity's equator. Specifically, in cases 1, 2, and 3, the mass flow increases with higher cryofan speed and pressure, while case 4 corresponds to a similar mass flow as in case 3, but at a higher pressure, placing it further from the supercritical point of the helium flow. From these plots, it is evident that case 3, with a pressure of approximately 3.5 bar, a cryofan speed of around 9500 rpm, and a mass flow of 125 mg/s ± 15-20%, demonstrates the most efficient performance. This case not only achieved the lowest cavity temperature of 6.50 K ± 20 mK at 1 W additional heat load but also exhibited the best cooling performance for the cavity. Specifically, from no introduced heat load to 1 W heat load, the T_{cavity} exhibited the smallest temperature increase of 0.8 K ± 15 mK. This temperature increase was measured relative to the increase in the T_{supply}, calculated as ΔT_{cavity} -ΔT_{supply}. In fact, the temperature of 6.50 K was achieved under different conditions, as shown in Figure 3 on the right, where case 2 also reached it. Furthermore, as mentioned previously, operating at higher pressures reduces heat transfer efficiency, as evident when comparing cases 3 and 4. Despite having similar mass flows, case 4, with its higher pressure, shows less efficient performance, reaching 7.40 K ± 20 mK at 1 W. In addition, Figure 3 on the left shows that the supply temperature also slightly increases with the introduction of the heat load, even though it is before the cavity. In order to stabilize the cavity's supply temperature and to further test the cooling performance of the cavity in detail, rather than the entire system, the use of the booster heat exchanger with the additional LHe bath is necessary.

4.2 Booster heat exchanger integrated operation

Measurements were taken at three different pressure levels: low (3/4 bar), medium (5/6 bar) and high (9/10 bar), alongside high cryofan speeds set at 16800 rpm, 17800 rpm, 18800 rpm, and 19800 rpm to achieve higher mass flow rates. Additionally, heating power settings ranged from 0 W to 3 W (7 W). Figure 4 depicts the temperature increase at the cavity's equator from 0 W to each heat load level, in respect to the "T_{inlet}" increase, which refers to the temperature of the flow at the inlet of the cavity, measured after the booster heat exchanger (Figure 1). This demonstrates the cooling performance of the cavity itself based on the chosen helium flow conditions. Figure 5 specifically depicts the temperatures achieved at the 3 W heat load level and it includes both the "T_{inlet}" and the "T_{cavity}" in relation to the mass flow for each pressure level case. Each data point is indexed and corresponds to the conditions listed in Figure 4's legend, where the labels for each point are provided.

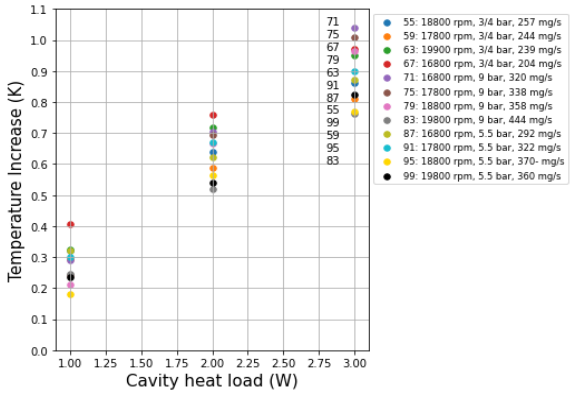

Figure 4. Cavity temperature increase from 0 W to each heat load.

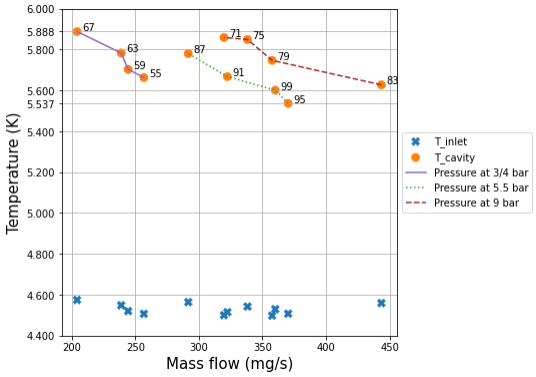

Figure 5. Cavity and inlet temperature at the 3 W heat load.

From these plots, it can be seen that point 95, characterized by a pressure of approximately 5.5 bar, a cryofan speed of around 18800 rpm, and a mass flow rate of approximately 370 mg/s ±15-20%, demonstrates the most efficient performance. This case not only achieved the lowest temperature at 3 W, reaching 5.54 K ± 20 mK, but also had a very good cooling performance for the cavity itself, exhibiting the smallest cavity temperature increase at 3 W, as depicted in Figure 4. In addition, points 83 and 99 also performed well. Overall, across all tested cases at 3 W, the temperature at the cavity's equator ranged between (5.54 K - 5.90) K ± 20 mK, while the temperature at the inlet to the cavity ranged between (4.50 K - 4.58 K) ± 20 mK. Furthermore, the use of the booster heat exchanger stabilized "T_{inlet}" to a maximum increase of 0.2 K from 0 W to 3 W. For the optimal case of point 95, additional experiments were conducted at higher heat loads of 5 W and 7 W to observe the resultant temperatures. From Figure 6 it can be seen that for no introduced heat load and with "T_{inlet}" of 4.35 K ± 20 mK, the cavity temperature reached 4.61 K ± 20 mK, indicating an estimated cavity residual heat load of approximately 1 W. When subjected to a 7 W heat load, the cavity temperature increased to 6.65 K ± 20 mK. An additional analysis was conducted for the aforementioned case to examine the local temperature increase across the entire length of the cavity at each heat load level up to 7 W. In Figure 2 on the right, the distribution and location of each temperature sensor on the cavity are depicted: T1, T2, T4, T6, and T8 (orange) are located on the capillary, while T3, T5, and T7 (grey) are located on the copper cavity surface. T_{inlet} is located on the inlet of the capillary, T_{outlet} is located on the outlet of the capillary and T_{cavity} is located on the equator of the cavity on a copper block. The analysis resulted in Figure 7, which depicts the temperature increase at each heat load for each of the temperature

sensors. It shows that the temperature increase over the length of the cavity remains below 50 mK up to 2 W heat load, and as the heat load increases, it becomes slightly more pronounced, reaching 220 mK at 7 W, as indicated by the dotted horizontal lines. However, this is relatively low, indicating that the copper effectively maintains an almost uniform temperature rise with added heat load.

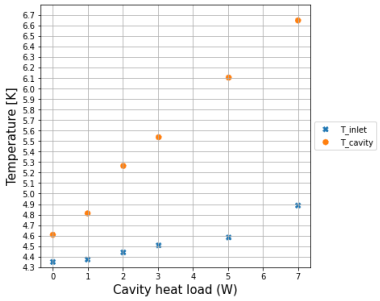

Figure 6. Cavity & inlet temperature at each heat load level for the case of point 95.

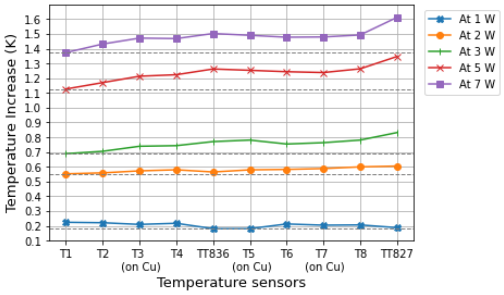

Figure 7. Temperature increase at each heat load level across all the temperature sensors of the cavity

5. Conclusion

This study investigates cryogenic dry cooling solutions for SRF cavities, presenting a promising alternative to traditional cooling methods. Numerical simulations and experimental validations assess heat transfer, temperature changes, and pressure drop characteristics in helium forced flow, providing insights into the system's performance. Single-phase helium flow was mainly studied, with pressures above supercritical conditions, particularly in the pressure range of 3 - 6 bar and 9 - 10 bar, and for mass flow rates between 80 - 450 mg/s ± 15-20%. The findings demonstrate the feasibility of remote cooling systems and the possibility to achieve low temperatures as required. In terms of system performance, the helium mass flow rate appeared to be the primary determining factor. During the standalone cryocooler operation, the cavity achieved a minimum temperature of 6.50 K ± 20 mK under an applied heat load of 1 W and with a residual heat load of approximately 1 W. To achieve a lower and constant inlet temperature, and consequently reduce the cavity temperature further with higher possible heat loads, an additional booster heat exchanger was integrated along with an additional 4.2 K liquid helium bath, enabling a more precise study of the cavity's cooling performance. In this case, the cavity achieved temperatures of around 5.50 K ± 20 mK under a 3 W heat load and 6.60 K ± 20 mK under a 7 W heat load. Additionally, an analysis of the local temperature increase along the entire length of the cavity was also conducted, showing that as the heat load increases, the temperature rise over the length of the cavity becomes more pronounced. For instance, under a 7 W heat load, the temperature increase across the entire length of the cavity was approximately 220 mK. However, this is relatively low, indicating that the copper effectively maintained an almost uniform temperature rise with added heat load. These innovative, reduced helium content cooling schemes hold promise for a wide range of superconducting cavity and magnet assemblies, with the potential to enhance low-temperature cooling capabilities and reduce the reliance on liquid cryogenic infrastructures.

References

[1] Onufrena A. et al., "Remote cooling systems with mesh-based heat exchangers for cryogenic applications", IOP Conf. Ser.: Mater. Sci. Eng. (2022).

[2] Padamsee, Hasan. "The Science and Technology of Superconducting Cavities for Accelerators." Cornell University, Ithaca, NY 14853, USA (2001).

[3] FasterCapital. "Superconducting Materials." FasterCapital, https://fastercapital.com/keyword/superconducting-materials.html.

[4] Onufrena A. et al., "Cryogenic performance of a compact high-effectiveness mesh counter-flow heat exchanger", Cryogenics (2022)